The objective of the present section of the study is to address the tasks of comprehensive analytical description of graphically synthesized holographic elements built according to diagrams and topologies of the AIRES New Medical Technologies Foundation, as well as synthesis and classification of possible forming patterns of transparencies with certain optical properties. Special attention in the data of this research was paid to the following question:

- what spatial multi-dimensional structures of spatial topologies make up the diagram graphics and, consequently, what three-dimensional structures can be synthesized with the aid of transparency sets that are aligned in space in a certain manner?

The performed theoretical analysis and experimental validation lead to the following basic conclusions.

Transparencies with Aires fractal-matrix graphics act as

- phase Fourier filters for spatial frequencies that single out the discrete frequency grid in that radiation, depending on the phase velocity *V* of particle streams or electromagnetic radiation going through or reflected by the transparencies,
- generators of an ordered raster structure governed by the main equation of Fraunhofer diffraction overlaid by a field structure of auto-reference of spatial frequencies connected to the fractalization centers in the strictly ordered points of the transparencies,
- graphically synthesized holograms that in coherent light generate the above-mentioned optical phenomena, and in non-monochromatic light they show a three-dimensional structure of 4 collimated beams of light intersecting in one point, with the internal filling of the light containing phenomena of «white» light dispersion.
- The latest results establish that fractal graphics in the zero center of fractalization is a conformal inverse mapping of regular net structures of a large number of second-order surfaces.

Based on the research findings, proposals for a whole range of investment projects were drafted to create technology of synthesis of especially pure materials (the «Especially Pure Materials» project), build optical systolic calculators and universal PCs, the project "Beta Converter. Principles of design of optical calculations and optical memory on the elements of fractal optics and fractal transparency optics, the project "Neutralizer. PC screen protector in the form of a fractal-matrix filter." Also, there are projects at the stage of proposal formulation for antenna-feeder devices, devices focusing different radiation, and a number of other proposals.

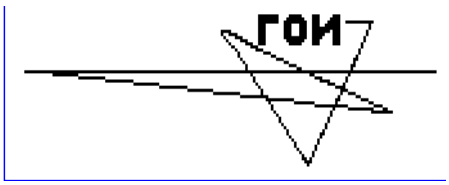

"Seen and approved"

Director General

"ALFA" CJSC

V.A. Osipov

"....."..... 2001

"Seen and approved"

Director General of the State Unitary Enterprise Russian Research Center

“S. I. Vavilov State Optical Institute"

member of the Russian Academy of Sciences

G.T. Petrovskiy

EXPRESS REPORT RECORD № 1

Stage 1

Development of optical systems and guidelines for making interferometric and polaroid devices with preset intensity distribution on transparency matrices with a high-density
fractal pattern.
Research work code – "Focusator"

“Approved”
Director of the State Unitary Enterprise
"State Optical Institute TKS-OPTIKA", Candidate of Technical Sciences

Ye.A. Iozep

Head of the Fundamental Research
Laboratory of Fractal Optics and Fractal
Transparency Optics: G.S. Melnikov

Saint Petersburg
2001.

Development of a Mathematical Model for Designing Transparencies with Fractal Graphics.

The objective of the present section of the research is to address the tasks of comprehensive analytical description of graphically synthesized holographic elements built according to diagrams and topologies of the AIRES New Medical Technologies Foundation, as well as synthesis and classification of possible forming patterns of transparencies with certain optical properties. Special attention in the data of this research was paid to the following question:

- what spatial multi-dimensional structures of spatial topologies make up the diagram graphics and, consequently, what three-dimensional structures can be synthesized with the aid of transparency sets that are aligned in space in a certain manner?

It became possible to set this objective when writing Reports № 2 and № 3 [1,2].

Report №3, section 2.5.2 (2) showed that normally most graphical diagrams following algorithms given in the article [3] can be reduced to the diagrams of equivalent diffraction gratings.

Thus, for example, due to representation of flat curves of inscribed and circumscribed squares as a triad of trigonometrical functions [1,2]

$$Sid_4\Omega \cdot p = \frac{Sin\Omega \cdot p + Sin_4\Omega \cdot p}{2} \qquad (3.1)$$

the geometric algorithm for designing an equivalent diagram of a fractal pattern will look as follows. This algorithm can be exemplified by an elementary formative pattern in one of fractalization centers (Fig. 3.2).

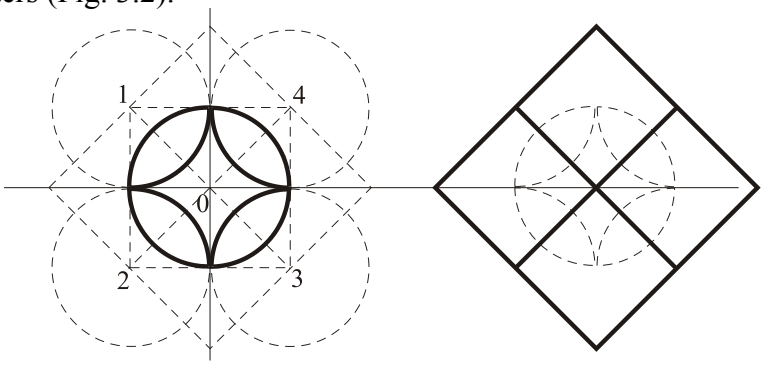

a) True elementary pattern b) Equivalent of an elementary pattern

Fig. 3.1.

Because the reading geometric wave ensures summation of intensity of the beams reflected from the mirror lines of the patterns, one can assert that the intersecting circumferences of the five neighboring fractalization centers (Fig. 3.1) have a double diffraction grating for a geometric equivalent (Fig. 3.3). (See Reports №1 and №2)

The Aires Foundation developed several types of fractal graphics deposited on different transparent substrates.

The bases of those transparencies usually are substrates for standard photographic masks with a size of 102 x 102 mm^2 $\Delta h = 2\ldots3$ mm; and the pattern in the form of concentric circumferences distributed on the field is deposited on mirror coatings by photolythography or contact exposure on a photoresist deposited on top of the mirror coating with subsequent etching of bright field sections.

The appearance and diagrammatic explanation of the transparency production technique are shown in Figs. 3.2 and 3.3

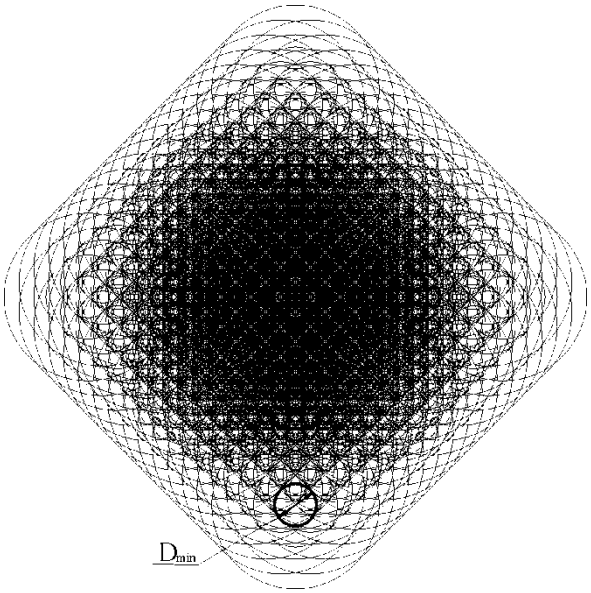

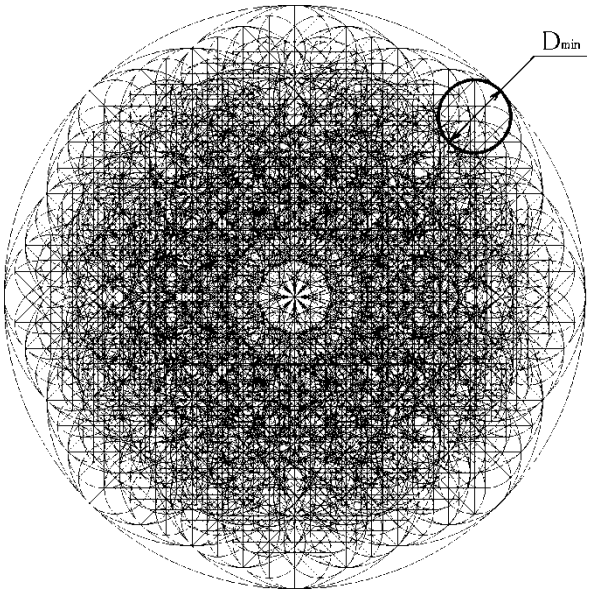

Fig. 3.2 **Fig. 3.3**

Figs. 3.2 and 3.3 show two-dimensional projections of four-level (n=4) modules, with k=4 and k=8 respectively, of a fractally assembled matrix of a filtering screen; Figs. 3.4... 3.6. show a diagram with the location of the modules on the substrate.

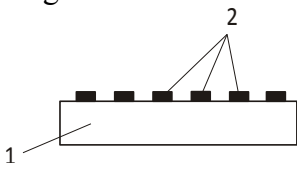

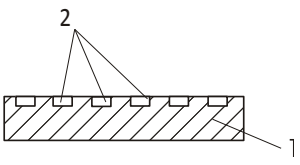

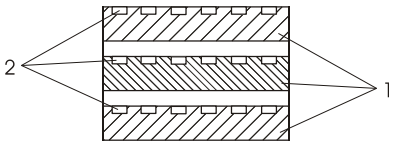

Fig. 3.4 **Fig. 3.5** **Fig. 3.6**

Figs. @@3.4–3.6 show the arrangement of the modules on the substrate in section. Fig. 3.6 shows a diagram of a transparency of several layers in section.

Because in the fractal structure of the graphics, the area of the transparencies displays a strictly hierarchical spatial orderliness, and the geometric wave of reading regularly queries meshy reflecting (conducting) sections of the graphics that repeat themselves on different scales, the question arises regarding possible detection of resonant (auto-interference) properties of those transparencies.

The experimental facts of the auto-interference phenomena observation are listed in Record 1 [18].

The present section of the Express Report Record will attempt to give a mathematical basis for this a number of other phenomena related to geometric configuration of fractal graphics, and therefore with the configuration of the geometric field of electromagnetic radiation reflected (conducted) by transparencies.

This is how this concept is described in the mathematics area studying configurations: configurations are spatial structures with ordered sets of points, lines and planes.

First of all, let us recall the main provisions of the geometric field of spatial frequencies that was introduced and substantiated by the author [11,12] based on the complete solution of the problem of mathematical billiards in a circle. The geometric field of spatial frequencies takes us to the notions of complex mapping of vector values in the internal (virtual) and external spaces of the studied objects, which characterize the vector values.

At the same time for the vector values, the surface (or rather its section) of multiple "reflections" of the vector values. As a rule, actual surfaces of reflection (D=0) are connected with the surface of the object in question or an element of the final configuration.

In this case, a vector value can be represented (in universal space) in a complex form

$$L_p(\Omega) = R\left(2\sin\frac{\pi}{k}\right)^D \cdot m(k,p)\cdot e^{\cdot i\cdot\frac{2\pi}{k}\cdot p} \tag{3.2}$$

- phase representation

or

$$L_p(\omega) = R\left(2\sin\frac{\pi}{k}\right)^D \cdot m(k,t)\cdot e^{i\cdot\frac{2\pi}{kn_{1,0}R}\cdot\frac{c}{(2\sin\pi/k)^D}\cdot t(D)} \tag{3.3}$$

- frequency representation

As equation (3.3) shows, the basic concept of the geometric field of spatial frequencies is taken as the spatial frequency concept

$$\omega_n = \frac{2\pi\cdot c}{n_{1,0}\cdot k\cdot R\cdot\left(2\sin\pi/k\right)^D} \tag{3.4}$$

That concept is directly proportional to the speed of light and inversely proportional to the length of the vector value of "multiple reflection" and the mode coefficient, i.e. the fractality coefficient.

The ratio $\frac{2\pi}{k}$ in the argument characterizes the mode or phase measure of the vector in the zero basis, which is a circumference with radius R of the multiple reflection of that vector.

The circumferences of mapping of the vector to the internal (virtual) space have discrete values of diameters

$$R_{-D} = R\cdot\left(2\cdot\sin\frac{\pi}{k}\right)^{-D}, \tag{3.5}$$

whereas the circumferences of mapping to the external space have discrete values

$$R_D = R\cdot\left(2\cdot\sin\frac{\pi}{k}\right)^{D} \tag{3.6}$$

Analysis of equations (3.3…3.6) shows that in space we deal with an infinite number of Riemann surfaces, i.e. nested concentric spheres. Here even values $D\in[-\infty,...0,...\infty]$ correspond to the spheres with rational radii, and uneven values characterize irrational radii of those spheres.

If indicator D is instilled with discrete-continuous nature of change, we will get a family of characteristics (Diagram 3.1.).

As the diagram shows, if the mode coefficients are 2 to 6, vectors 3.6. are mapped to the external space. With the fractality coefficient k=6, the vectors are mapped to circumferences with radius R, in the simulation experiment (R=2).

Mapping of vectors that have mode fractality coefficients > 6 is performed to the internal (inverse space) of the sphere with a real radius (R=2) .

$R_D(k,D,R)$

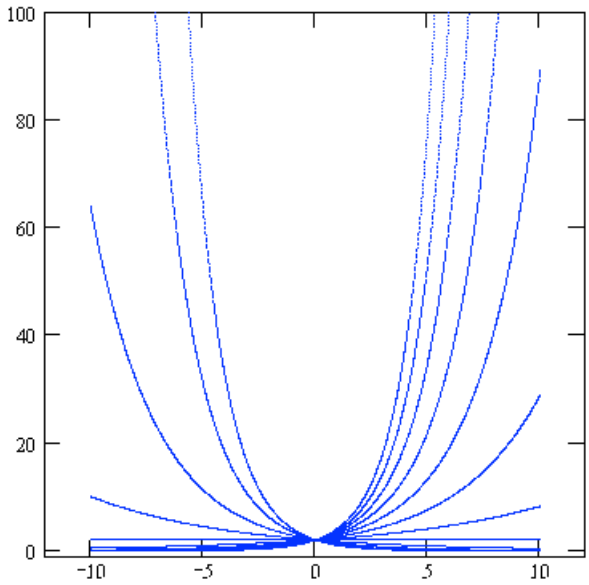

Diagram 3.1. The family of characteristics $R_D(k,D,R)$ as a function of the current values of indicator D simulated in Math Cad 2000 using expression 3.8.; with the values of the mode fractality coefficient $k \in [2,3\ldots13]$.

Let us take dependency of the amplitude-phase multiplier m(k,p) on the current values of

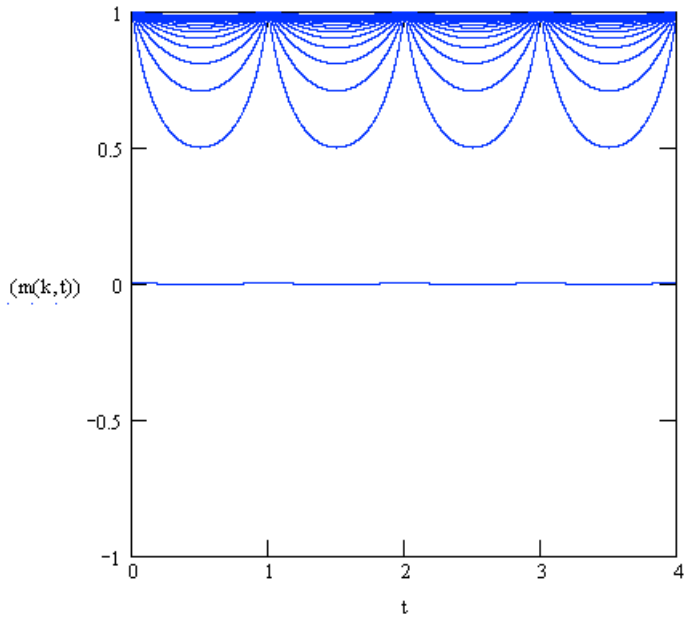

parameter *p*

Diagram 3.2. The family of characteristics m(k,t) as a function of the current values of time t simulated in Math Cad 2000.

In this case, for k=2.3…8 the curves successively shift from the lines in the area of level 0 to 1.

On the whole, according to equation 3.2., vector $L_p(\Omega)$, with integer-valued changes of *D*, will be mapped to the external and internal space as discrete spiral mappings. With the current changes of indicator *D*, that mapping appears as smooth right-hand and left-hand spirals, see Diagrams 3.3 and 3.4.

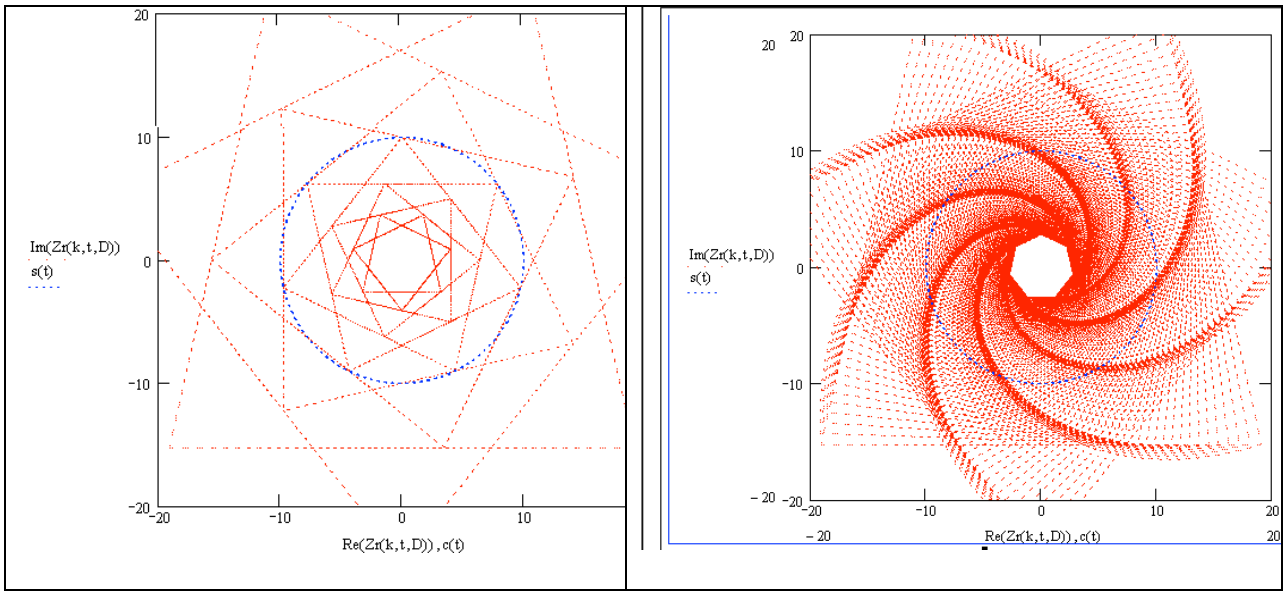

Diagram 3.3. Diagram 3.4.

Discrete and discrete-continuous mappings of a vector with the submode fractality coefficient k=7/2 to external and internal space of a sphere with radius R=10 (meridian section)

The performed theoretical analysis and experimental validation obtained in the Record [18] lead to the conclusions [19] that the synthesized transparencies act as:

- Fourier filters of spatial frequencies,
- generators of an ordered raster structure governed by the main equation of Fraunhofer diffraction overlaid by a field structure of auto-reference of spatial frequencies connected to the fractalization centers in the strictly ordered points of the transparencies,
- graphically synthesized holograms that in coherent light generate the above-mentioned optical phenomena, and in non-monochromatic light they show a three-dimensional structure of 4 collimated beams of light intersecting in one point, with the internal filling of the light containing phenomena of «white» light dispersion [18].
- The latest results obtained by the authors establish that fractal graphics in the zero center of fractalization is a conformal inverse mapping of regular net structures of a large number of second-order surfaces.

Comparison of the device in development with the existing notions of the electromagnetic oscillation theory.

Let us consider four basic provisions from the wave function theory.

First of all, let us define the notion of the phase plane according to [15]

Phase plane method [15] (page 78)

If processes occurring in a system are fully described by specifying two variables x and y, then they can be rendered in a Cartesian coordinate system. The plane (x, y) is called a phase plane ("phase" here means "state"), and a phase plane is the plane of the system's states, and each point is a representation point.

Because x and y are functions of time x=x(t) and y=y(t), with the course of time the representation point describes a curve on the phase plane that is called a phase trajectory.

The aggregate of phase trajectories corresponding to different values of the initial conditions is called the system's phase portrait.

Study of the behavior of phase trajectories helps answer a number of important questions that cannot be solved by a whole range of existing rules of thumb. Particularly, studying the system's operation in a phase plane helps identify possible types of oscillations in this system with different values of the initial conditions and evaluate stability of the states of equilibrium and periodic motion "in the large," i.e. if there are any great excitations.

If the system is described by not two but three variables (a third-order system) etc. n variables, then its behavior can be studied in the phase spaces x, y, z or X, Y, Z, … N of the wave vector according to [16]:

A wave vector is the vector $K = (k_1, .. k_m)$ included in the equation $a \cdot \exp\left(i \sum_{j=1}^{m} k_j x_j - i\omega t \right)$ (3.7)

Where a and ω are constants, t is time

In physical terms, equation (3.10) is usually interpreted as a plane wave with frequency ω propagating towards vector K with wavelength

$$\lambda = 2\pi / K \quad (3.8)$$

Many homogeneous linear equations and simultaneous equations with partial derivatives (including crucial equations of mathematical physics, for example, Maxwell's equations, wave equations) admit solutions in the form of (3.7).

Fourier series

If the examined periodic function $f(t)$ is specified in the finite interval, it can be broken into a Fourier series. If we take the interval $\left[-T/2, +T/2 \right]$ without prejudice to affinity, we have the series

$$f(t) = A_0 + \sum_{n=1}^{\infty} \left(A_n \cos\left(\frac{2\pi \cdot n}{T} \cdot t \right) + B_n \sin\left(\frac{2\pi \cdot n}{T} \cdot t \right) \right) \quad (3.9)$$

$$A_0 = \frac{1}{T}\int_{-T/2}^{T/2} f(t)dt$$

where

$$\left.\begin{aligned} A_n &= \frac{2}{T}\int_{-T/2}^{T/2} f(t)\cdot\cos\frac{2\pi\cdot n}{T}\cdot t\cdot dt \\ B_n &= \frac{2}{T}\int_{-T/2}^{T/2} f(t)\cdot\sin\frac{2\pi\cdot n}{T}\cdot t\cdot dt \end{aligned}\right\} \qquad (3.10)$$

are real coordinates, the so-called harmonic amplitudes $n\omega_0 = \frac{2\pi\cdot n}{T}$

It is more convenient to use the complex modification of the series

$$f(t) = \sum_{n=-\infty}^{\infty} C_n \cdot e^{i\frac{2\pi\cdot n}{T}\cdot t} \qquad (3.11)$$

$$C_n = \frac{1}{T}\int_{-T/2}^{T/2} f(t)\cdot e^{-i\frac{2\pi\cdot n}{T}}\cdot dt \qquad (3.12)$$

where

are complex coefficients that with real function $f(t)$ have property $C_n = C_{-n}^{*}$ (* means complex contingency)

Fourier transform [3]

With an infinite range of values of t, the series (3.9 and 3.11) is replaced with a Fourier integral, i.e. integral expression,

$$f(t) = \frac{1}{2\pi}\int_{-\infty}^{\infty}\Phi(i\omega)\cdot e^{i\omega t}\cdot d\omega \qquad (3.13)$$

inverse to which is the Fourier transform

$$F\{f(t)\} \equiv \Phi(i\omega) = \int_{-\infty}^{\infty} f(t)\cdot e^{-i\omega t}\cdot dt \qquad (3.14)$$

The complex function $\Phi(i\omega)$ is called a Fourier spectrum or Fourier transform $f(t)$

Below is an overview of the main properties of a Fourier transform:

1) Linearity

$$\begin{aligned} F\{f_1(t)+f_2(t)\} &= F\{f_1(t)\}+F\{f_2(t)\} \\ F\{af(t)\} &= aF\{f_1(t)\}+F\{f_2(t)\} \end{aligned} \qquad (3.15)$$

2) Linear scaling

$$F\{f(at)\} = \frac{1}{a}\Phi\left(\frac{i\omega}{a}\right) \qquad (3.16)$$

3) Shift of the original

$$F\{f(t-\tau)\} = F\{f(t)\}\cdot e^{-i\omega\tau} \qquad (3.17)$$

4) Shift of the spectrum

$$F\{f(t)\cdot e^{at}\} = \Phi(i\omega + a) \qquad (3.18)$$

5) Roll-up of transforms

$$F\{f_1(t)\cdot f_2(t)\}=\frac{1}{2\pi}\int_{-\infty}^{+\infty}\Phi_1(i\omega')\cdot\Phi_2(u(\omega-\omega'))\cdot d\omega' \tag{3.19}$$

6) Roll-up of originals

$$F\left\{\int_{-\infty}^{\infty}f_1(\tau)\cdot f_2(t-\tau)d\tau\right\}=F\{f_1(t)\}F\{f_2(t)\} \tag{3.20}$$

7) The rule of the derivative

$$F\{f'(t)\}=i\omega F\{f(t)\} \tag{3.21}$$

8) Parseval's Theorem

$$\int_{-\infty}^{+\infty}f^2(t)dt=\frac{1}{2\pi}\int_{-\infty}^{+\infty}|\Phi(i\omega)|^2 d\omega \tag{3.22}$$

To the left stands energy of the signal whose component parts are grouped along the time axis, to the wright – along the frequency axis.

Fractal graphics is represented on Aires transparencies by means of complex parametric equations of type (3.3); they ensure successful interpretation of that graphics using the above-mentioned basic provisions of the wave function theory.

First of all, let us point out that fractal-matrix transparencies themselves can be treated as phase planes on which Fourier filtration of streams of different electromagnetic oscillations is performed.

Indeed, if the fractal graphics is approached from a system perspective, it becomes quite obvious that the dynamics of designing the graphics by means of equations (3.2) can be interpreted as mapping of processes characterizing certain systems by specifying two variables, x and y.

At the same time, analysis of equation (3.2) shows that each of the parametric equations, into which this complex-valued composite function can be broken, in turn depends on a number of other parameters, both discrete and continuous. It is not difficult to see that parameter p in (3.2), i.e. the current value of the points of mapping the equivalent basic vector L is replaced in the following equation

$$p=\frac{V}{R_0 n_{1,0}\cdot\left(2\sin\pi/k\right)^p}\cdot t \tag{3.23}$$

that is, x and y are functions of time, and the dynamics of filtration processes of the resulting phase graphics (3.2) will be in this case characterized by speed V.

Quite obviously, the introduced speed V is a basic physical quantity characterizing spatial-frequency properties of the Fourier phase filter, in which capacity transparencies with fractal-matrix graphics are used. Equation (3.23) shows with what frequency the query of the parameter p will change per unit of time t, as any stream (gravitational flow, electron stream, sonic flow, electromagnetic flow) with a phase velocity V goes through the transparency. And consequently, for each of the listed radiation flows, a discrete sequence (D) of spatial frequencies can be calculated, on which this Fourier filter will have resonance properties.

In equation (3.4) written for electromagnetic oscillations, the speed is taken as the speed of light, and consequently, the filter with the graphics given in Fig. 3.7, with R_0 = 5,1875 mm, with D=0 and three levels of fractalization, will have four resonance frequencies.

In that presentation, the graphics of the transparencies turns from the phase plane (phase mapping) to spatial-frequency plane of Fourier transforms.

Let us consider the general characteristics and differences in rendering fractal-matrix graphics from the perspective of the notion of "wave vector" from the points of view of wave and spatial-frequency presentation of the geometric field equation.

Let us also look again at equations (3.9…3.12) used for rendering the periodic function $f(t)$ by expanding it in a Fourier series, as well as at equations (3.13…3.22) used for rendering $f(t)$ with an infinite range of values t.

Comparison of the equations

$$n\omega_0 = \frac{2\pi n}{T} \tag{3.24}$$

$$n\Omega_{\Pi} = \frac{2\pi}{k} \tag{3.25}$$

as well as

$$\omega_p = \frac{2\pi}{k} \cdot \frac{C}{R_0 n_{10} \left(2\sin \pi/k\right)^{\infty}} \tag{3.26}$$

demonstrates similarity and differences between the wave description of the function $f(t)$ and the spatial-frequency description following from the description of the geometric field of spatial frequencies.

At first glance, equations (24) and (25) are the same representation. Moreover, with the fractality coefficient represented as rational numbers $k = \frac{n}{m}$

$$\Omega_{\Pi} = \frac{2\pi m}{n} \tag{3.27}$$

(where m and n are positive integers, where $n \in [2,3,...,\infty]$ $m \in [0,1,...,\infty]$), the similarity between equations (24) and (25) is even stronger.

An even stronger comparison suggests itself

$$\Omega_{\Pi} = \frac{2\pi}{k} \tag{3.28}$$

with a familiar rendering of the wave vector as a plane wave with frequency ω propagating towards vector K with wavelength

$$\lambda = \frac{2\pi}{K} \tag{3.29}$$

where $K = k(k_1, k_2, ..., k_m)$

Moreover, comparing equations (3.4) with the equation that is familiar from the electromagnetic field theory [17] and introduced by simplification, the so-called "symbolic method', i.e. the method of complex amplitudes using Euler's formula:

$$e^{j(\omega t+\varphi)} = \cos(\omega t + \varphi) + j\sin(\omega t + \varphi) \tag{3.30}$$

enforces even further the similarity with the geometric field equations of spatial frequencies.

However, despite the great similarity of these instruments of describing wave processes, they have the following significant differences:

1. The symbolic method of the known field manipulates the inverse trigonometric functions.

The method of describing the geometric field of spatial frequencies uses the triad of complex trigonometric functions:

a. the inverse trigonometric functions (for which the end of the radius-vector follows the circumference from the center of coordinates the same way as in the electromagnetic field theory)
b. non-inverse trigonometric functions (for which the end of the radius-vector follows regular closed or open inscribed (or circumscribed polygons))
c. inverse circular – discrete trigonometric functions, (for which the end of the radius-vector follows astroid-like inverse discrete mappings of the circumference within the circle). The arcs of the astroid-like inverse circumference are made up by vectors whose beginnings are in the apexes of the circumscribed regular polygons.

2. In the familiar electromagnetic field theory, the phase plane and the frequency plane are absolutely different planes.

In the theory of the geometric field of spatial frequencies, the phase plane and the frequency plane are the same plane, except when describing the processes in the frequency plane, the harmonic processes are characterized through different velocities of propagation of the vector value on mathematical billiards trajectories in the inverse space of the circle.

3. The harmonic analysis of the familiar theory of electromagnetic field is expansion of the periodic function as a Fourier frequency spectrum.

On the contrary, harmonic analysis in the theory of the geometric field of spatial frequencies represents a periodic function as a sum of complex harmonic constituents (mode, sub-mode and stochastic) of the phase expansion of those functions.

The above analysis shows that the machinery of a geometric field of spatial frequencies, being based on exact solution of the mathematical problem of billiards in a circle, describes not integral energy characteristics, i.e. material characteristics of electromagnetic fields, but structural characteristics of the topology of spatial objects (both of internal spaces and external spaces, (inverse spaces of objects)).

A geometric field of spatial frequencies is a structure-forming field – a field of directions, whose hyper-complex mappings can describe the main characteristics of known electromagnetic fields, as well as external and internal structural properties of objects of universal space at macro- and micro-levels. Let us establish those assertions as exemplified by analysis and synthesis of fractal-matrix graphics from the point of view of a geometric field of spatial frequencies, the theory of partition of planes and space.

Correctness of the developed model of describing transparencies with a high-density fractal pattern, in the author's opinion, is fully confirmed by the graphic experiment with isolation of fractalization centers (see, centers of origin of «spherical» waves of the geometric field of spatial frequencies), which were made by collapsing the graphic analog of Fresnel zone plate with the raster structure of pixel-by-pixel rendering of the graphics on an HD monitor.

This can be demonstrated in Fig. 3.6, which shows the results of the graphic synthesis of the origin of interference fringe patterns on a PC monitor [1].

Figure 3.7 was made via Print Screen. The screen of the monitor in use is a high resolution digital monitor with a large number pixels on the screen (in this case, the 1024 x 768 resolution was used), and the test object is the scanned image of the Fresnel zone plate whose size decreases twofold in each field of the image.

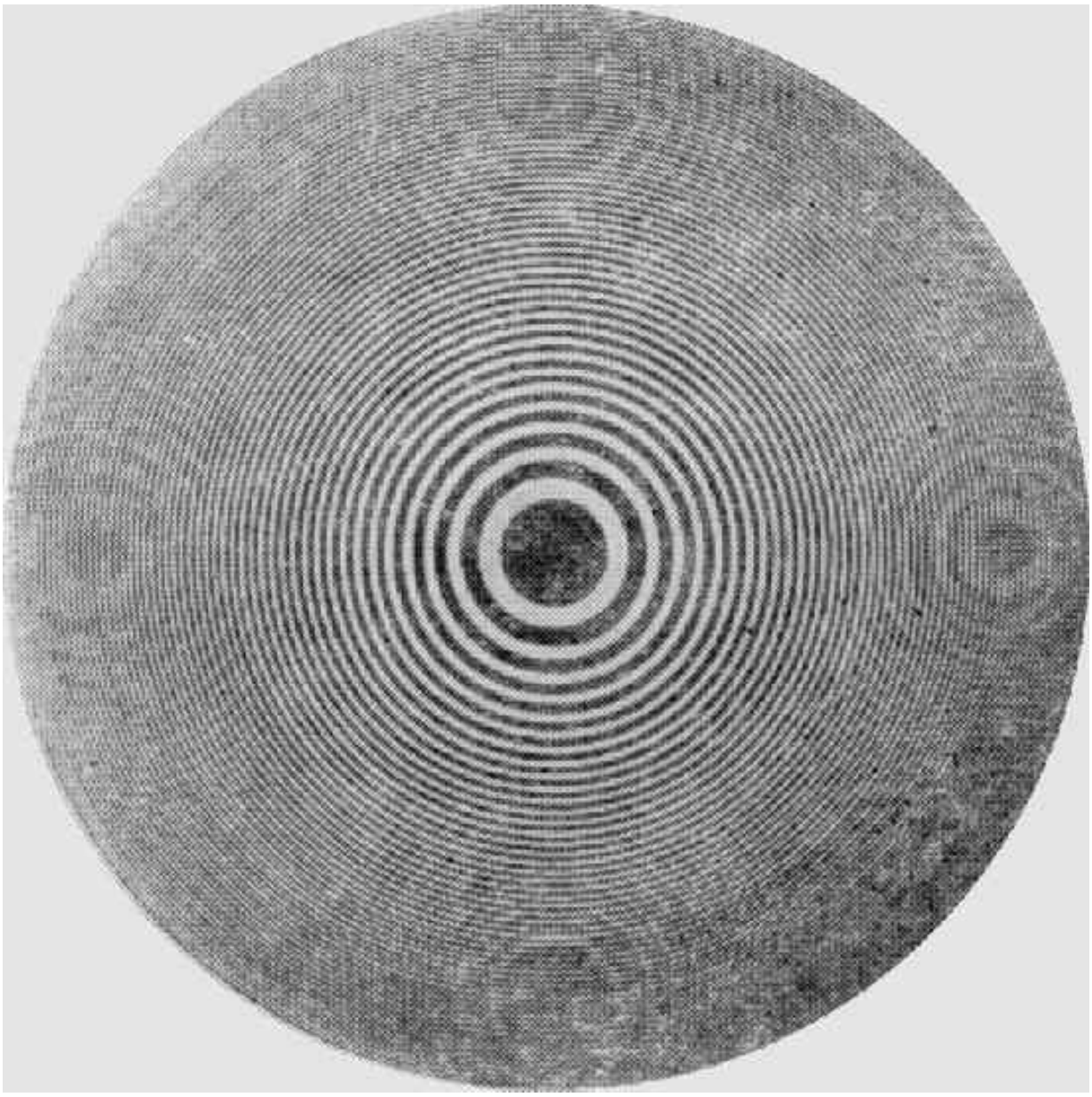

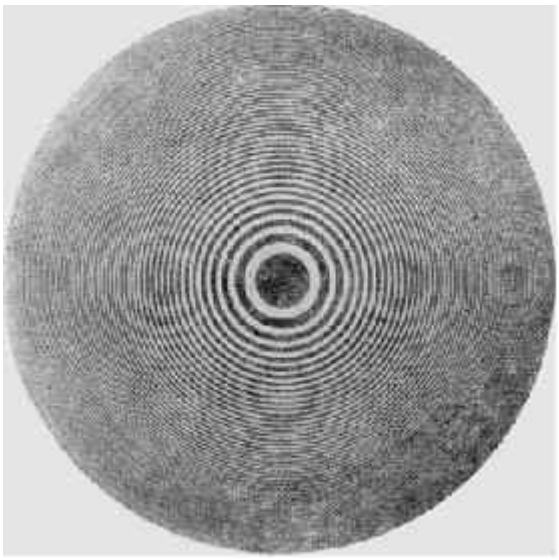

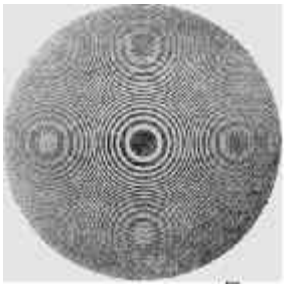

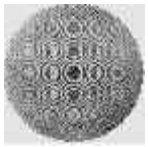

Fig. 3.7.

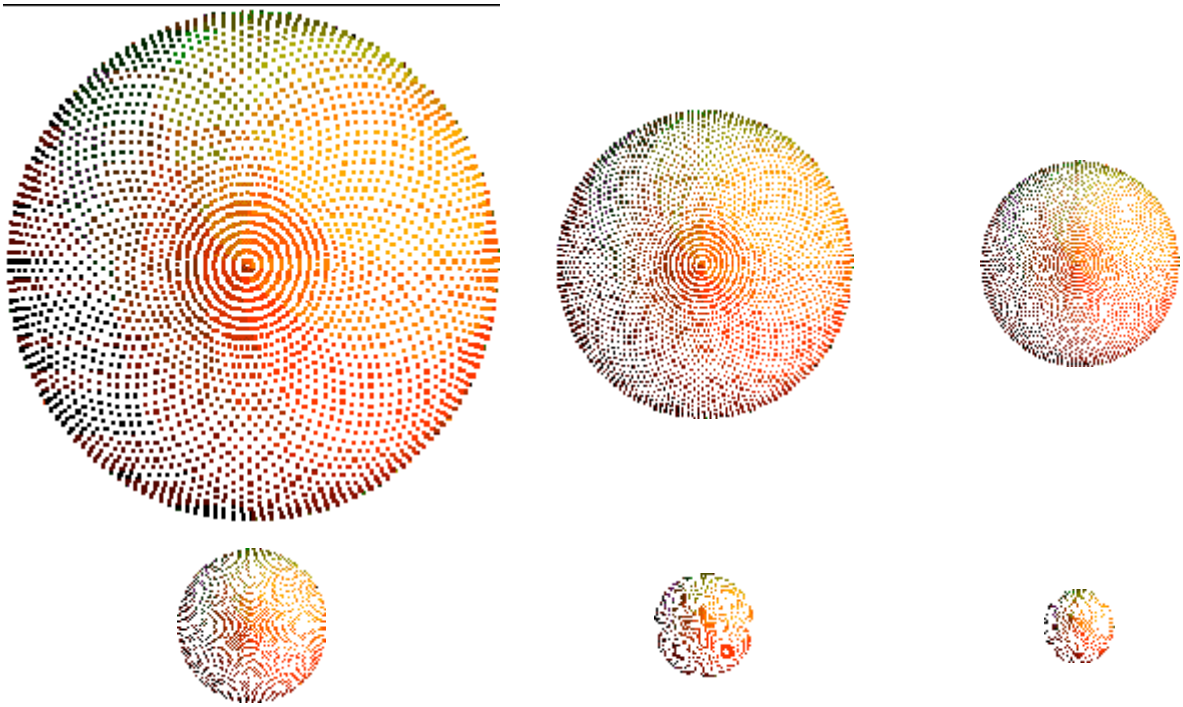

Fig. 3.8.

These figures show the results of collapsing of the graphics of of macro-scaled templates of the Fresnel zone plate and the basic fractal graphics of transparencies with mesh equivalents of the raster pixel-by-pixel resolution of the PC monitor.

The graphics of other ZX and ZY projections will have similar properties listed on pages…. On the whole, spatial interaction of the three complex mappings of spatial frequencies that physically act as an amplitude-phase modulation of light fluxes with a specified structural configuration of synthesized three-dimensional structures can ensure generation of specified configurations and structures of space.

These phenomena can be interpreted as follows.

A pattern of a Fresnel zone plate on different scales of its manifestation interacts, in visual perception, with the space lattice of line-pixel screen resolution.

We have demonstrated how a system of fractal circumferences can be reduced to a regular equivalent in the form of a grid of straight lines.

As a result, the ordered set of centralized spatial frequencies interacts with distributed sources of spatial frequencies.

$$\omega_{Пэкрана} = \frac{\pi C}{4 \cdot \delta \cdot \sin \pi / \ 4} \qquad (3.31)$$

where δ is the radius of the circumferences describing the monitor's pixel.

If, similarly to the description of this computer-aided experiment, the size of the basic pattern of fractal transparencies changes not in a binary progression but, for example, in an arbitrary geometric progression,

$$\rho = RK^n \qquad (3.32)$$

where K denotes integers, then the construction diagrams will be significantly different, which is the subject of study in the present section of the express report record
of the fractal transparencies

The inferred equations of the geometric field of spatial frequencies were simulated in MathCAD 2000 as the following program units:

$$Zdis(k,p,q,R) := R\cdot\left(2\cdot\sin\left(\frac{\pi}{4}\right)\right)^{(q)}\cdot\left[e^{i\cdot\left(\frac{\pi}{4}\cdot floor(p)\right)}+(m(2\cdot k,p\cdot k)\cdot e)^{i\cdot\left[\frac{2\cdot\pi}{4}\cdot(2\cdot k\cdot p-1)+q\cdot\frac{\pi}{2}+(1-q)\cdot\pi\cdot 4\right]}\right] \tag{3.33}$$

which ensured construction of equivalent diagrams and initial basic patterns representing a modification of the Customer's Diagram 3 for equations (3.2)

(Figs. 3.9…3.10)

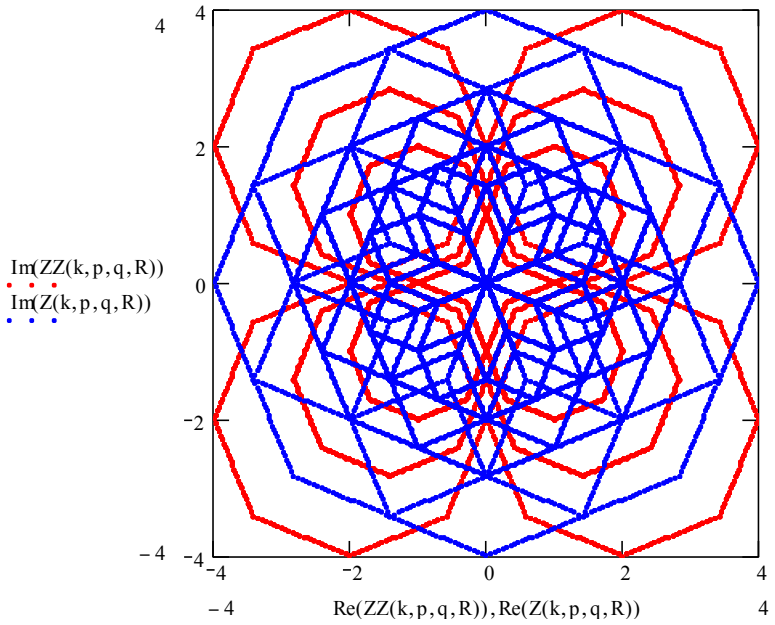

Fig. 3.9. The diffraction equivalent of Diagram 3 modified by the zero center of fractalization according to equations (3.2).

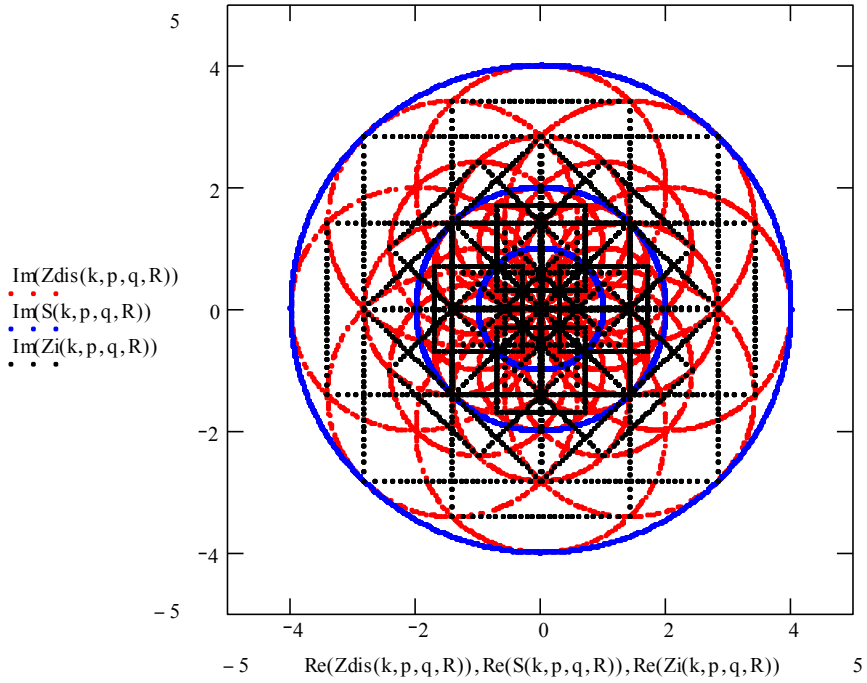

Fig. 3.10. Diagram 3. of the Customer modified by the zero center of fractalization according to equations (3.2).

Also implemented are a full graphic equivalent in the form of intersecting diffraction gratings and an analytical function describing the Customer's Diagram 3 by the zero center of fractalization according to the algorithm approved by the Customer.

These findings are presented as a program unit (3.34), and images of diagrams designed according to this program unit are given in Figs. 3.1 and 3.12. By the zero center of fractalization

по нулевому центру фрактализации

$$Z(k,p,q,R) := R \cdot 2^{(q)} \cdot [\,[\,A(k,p) + (m(k,p \cdot 2 \cdot k)) \cdot B(k,p \cdot 2 \cdot k)\,]\,]$$

$$ZZ(k,p,q,R) := R \cdot 2^{(q)} \cdot [\,C(k,p) + (m(k,p \cdot k)) \cdot E(k,p \cdot k)\,]$$

$$Zinv(k,p,q,R) := R \cdot 2^{(q)} \cdot \left[\left[e^{i \cdot \frac{\pi}{4} \cdot floor(p)} \right] + \left[e^{i \cdot \left[\frac{2 \cdot \pi}{4} \cdot (p \cdot k) \right]} \right] \right] \qquad (3.34)$$

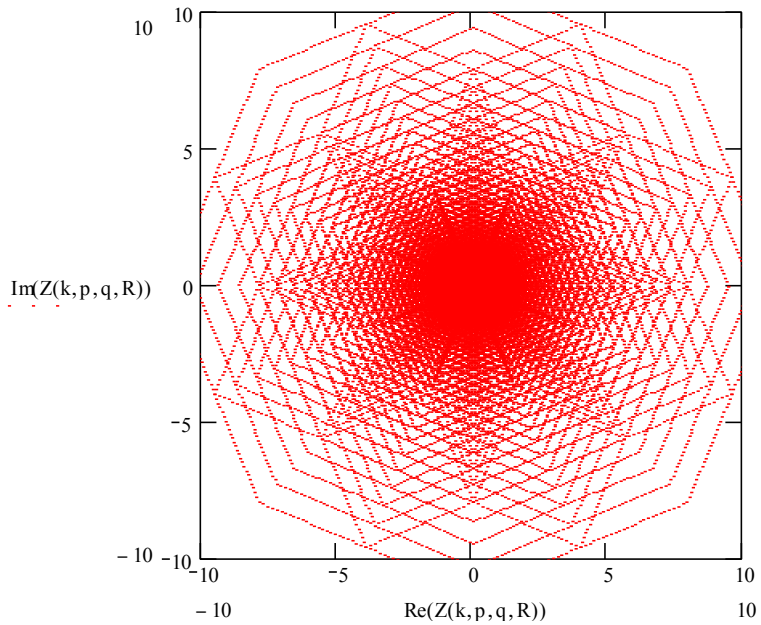

Fig. 3.11. Full diffraction equivalent of Diagram 3 modified by the zero center of fractalization according to the Customer's algorithms

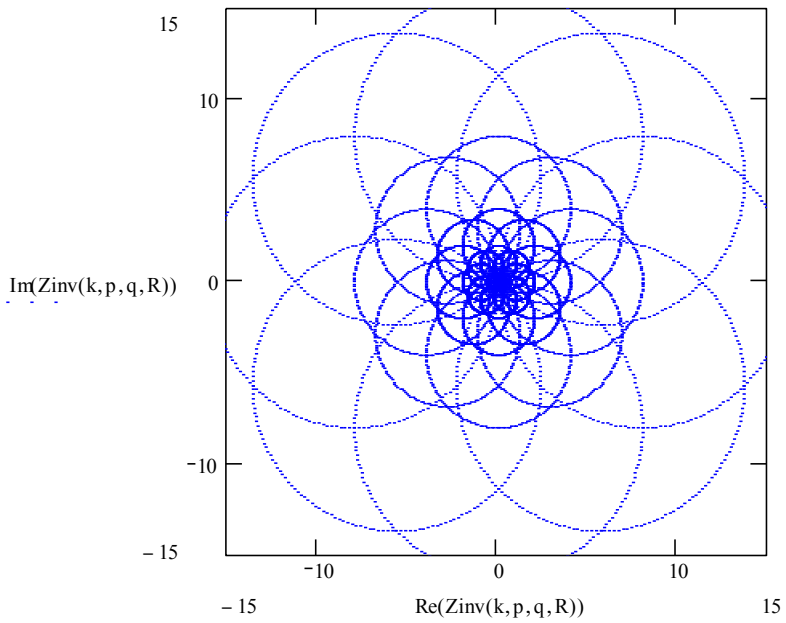

Fig. 3.12. Diagram 3 of the Customer modified by the zero center of fractalization according to the Customer's algorithms

In the course of mathematic simulation when presenting equations (3.34) in matrix form and specifying them in the XYZ coordinate system, it was successfully demonstrated that the Customer's graphic diagrams (topologies), as they are described analytically by fractional rational functions, have (are) conformal mappings on curved surfaces of three-dimensional topological structures originating from the Customer's basic fractal patterns.

This proof provides a fundamentally new approach to possible development of work on using the Customer's transparencies to create holographic assemblies of transparencies with fractal graphics for specific synthesized three-dimensional topologies of spatial objects. The

results of simulation of engendering (engendered) spatial structures and their multi-dimensional shells are given in APPENDIX 1 to Ch. 3 (proposals to the Crystal project).

As it turns out, the Customer's fractal graphics is not a section of some three-dimensional structure, but a conformal mapping. i.e. a projective view of a multi-dimensional topology along (towards) the Z-axis.

During mathematical simulation, apart from the above-mentioned cardinal conclusion, it was established and demonstrated that although the Customer's diagram solutions (Diagrams 2,3, 2-bis) are built intuitively according to strictly harmonized structures (wherein the diagrams are based on topological structures with equal real and imaginary vectors of spatial frequencies), they still do not cover even a small portion of possible and fundamentally necessary diagram topologies that will be used to solve the problems of focusing light fluxes on sets of diffraction transparencies with specified distribution of intensity on a focal plane.

Examples of other diagram topologies are given in Table 3.4

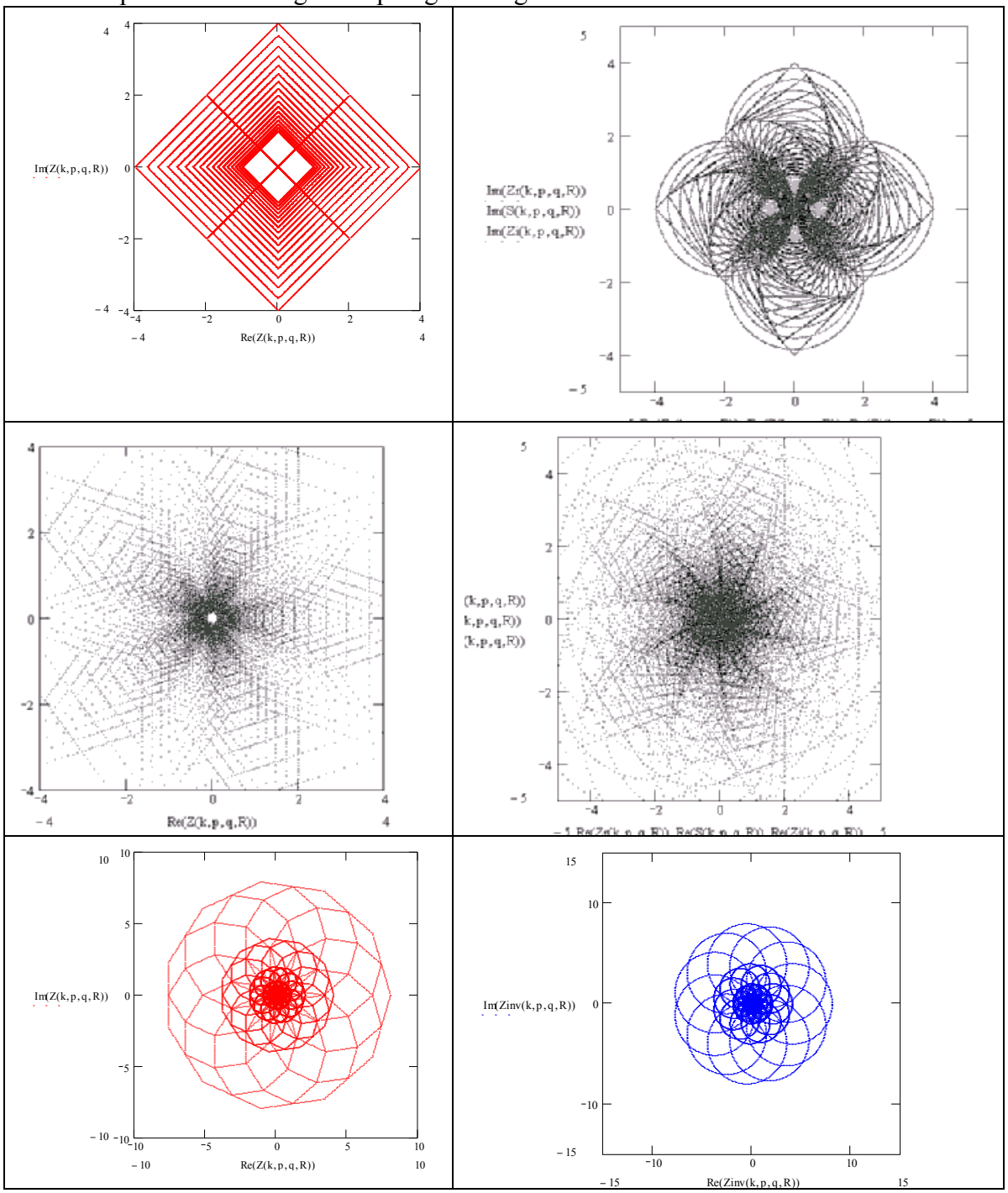

Let us consider a number of practical applications of the drawn conclusions.

Conclusions.

The performed theoretical analysis and experimental validation obtained in the Record [18] lead to the following basic conclusions.
Transparencies with Aires fractal-matrix graphics act as

- phase Fourier filters for spatial frequencies that single out the discrete frequency grid in that radiation, depending on the phase velocity V of particle streams or electromagnetic radiation going through or reflected by the transparencies,
- generators of an ordered raster structure governed by the main equation of Fraunhofer diffraction overlaid by a field structure of auto-reference of spatial frequencies connected to the fractalization centers in the strictly ordered points of the transparencies,
- graphically synthesized holograms that in coherent light generate the above-mentioned optical phenomena, and in non-monochromatic light they show a three-dimensional structure of 4 collimated beams of light intersecting in one point, with the internal filling of the light containing phenomena of «white» light dispersion [18].
- The latest results establish that fractal graphics in the zero center of fractalization is a conformal inverse mapping of regular net structures of a large number of second-order surfaces.

Based on the research findings, proposals for a whole range of investment projects were drafted to create technology of synthesis of especially pure materials (the «Especially Pure Materials» project), build optical systolic calculators and universal PCs, the project "Beta Converter. Principles of design of optical calculations and optical memory on the elements of fractal optics and fractal transparency optics, the project "Neutralizer. PC screen protector in the form of a fractal-matrix filter." Also, there are projects at the stage of proposal formulation for antenna-feeder devices, devices focusing different radiation, and a number of other proposals.